Acta Crystallographica Section F
Structural Biology and Crystallization Communications
ISSN 1744-3091

Crystallization and preliminary X-ray crystallographic study of the human MST2 SARAH domain

Jinsue Song,[a] Hyerim Hong,[a] Saehae Choi,[a] Yong Hee Lee,[b] Eiki Yamashita,[c] Suk-Chul Bae,[b] Il Yeong Park[a] and Soo Jae Lee[a]*

[a]College of Pharmacy, Chungbuk National University, Cheongju 361-763, Republic of Korea, [b]Biotechnology Research Institute, Chungbuk National University, Cheongju 361-763, Republic of Korea, and [c]Institute for Protein Research, Osaka University, 3-2 Yamada-oka, Suita, Osaka 565-0871, Japan

Correspondence e-mail: sjlee@chungbuk.ac.kr

Received 18 July 2011
Accepted 18 August 2011

The SARAH domain at the C-terminus of human MST2 (residues 436–484) was overproduced and purified using an *Escherichia coli* expression system. The purified domain was crystallized using the hanging-drop vapour-diffusion technique. Two crystal forms were obtained. The crystals belonged to space group $P2$, with unit-cell parameters a = 62.0, b = 119.2, c = 62.0 Å, α = 90.0, β = 90.5, γ = 90.0°, or to space group $P6_122$, with unit-cell parameters a = 54.5, b = 54.5, c = 303.1 Å. These crystals diffracted to 2.7 and 3.0 Å resolution, respectively.

1. Introduction

Mammalian sterile 20-like kinases 1 and 2 (MST1 and MST2) are core components of the Hippo signalling pathway, which plays a crucial role in cell proliferation and apoptosis (Wu *et al.*, 2003). MST1 and MST2 share 78% sequence identity (Creasy & Chernoff, 1995). MST kinase activity can be regulated by caspase cleavage of the C-terminal inhibitory domain (Graves *et al.*, 1998), resulting in translocation of the kinase domain to the nucleus. In response to apoptotic stress, MSTs can induce phosphorylation of histone H2B and activation of JNK, leading to chromatin condensation, DNA fragmentation and apoptosis (Bao *et al.*, 2011). Autophosphorylated MST1/2 interacts with Salvador (Sav)/WW45 for translocation into the nucleus to activate LATS1/2 (Chan *et al.*, 2005), which results in the downregulation of transcription factors *via* phosphorylation and inactivation of YAP (the transcription coactivator yes-associated protein). YAP has been shown to play a key role in mediating cell-contact inhibition, organ size and tumourigenesis (Zhao *et al.*, 2007). The C-terminal region of MST1/MST2 contains a SARAH (**Sa**v/**RA**SSF/**H**ippo) domain that interacts with the corresponding SARAH domain of WW45 (Callus *et al.*, 2006). The SARAH domain mediates a heterotropic interaction that transmits the signal from MSTs through the scaffolding protein WW45 to the downstream component LATS1/2 (Scheel & Hofmann, 2003). In addition, MST1/2 dimerize *via* the SARAH domain (Creasy *et al.*, 1996) and the auto-activation of MST1 is inhibited by removal of the SARAH domain (Lee *et al.*, 2008). Thus, SARAH-mediated homodimerization and heterodimerization induces apoptosis and suppresses cell-cycle progression (Scheel & Hofmann, 2003).

A previous study of the solution structure of the human MST1 SARAH domain revealed its homodimeric structure and its heterotropic interaction with the Rassf5 and WW45 SARAH domains (Hwang *et al.*, 2007). To identify structural features of the MST2 SARAH domain and provide further information on the molecular mechanisms of the Hippo pathway, we performed the overproduction, purification, crystallization and preliminary X-ray diffraction data analysis of the MST2 SARAH domain.

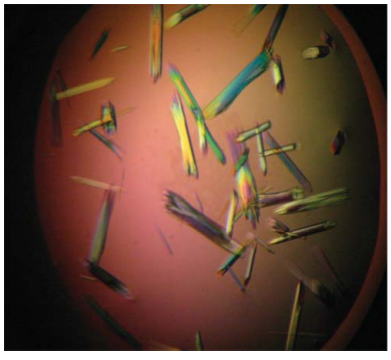

2. Materials and methods

2.1. Cloning, overproduction and purification

The cDNA coding the MST2 SARAH domain (residues 436–484) was subcloned into a modified pGEX4T1 vector (GE Healthcare,

USA) containing an N-terminal GST tag and a tobacco etch virus (TEV) protease-cleavage site. The nucleotide sequence was verified by DNA sequencing. The resulting construct was transformed into *Escherichia coli* BL21 (DE3) strain for protein overproduction. The transformed cells were cultured in LB medium containing 100 µg ml^{-1} ampicillin at 310 K until the OD_{600} reached 0.5–0.6. Target-protein overproduction was then induced by incubating the cells with 0.3 m*M* IPTG at 291 K for 16 h. The cells were harvested by centrifugation at 6000*g* for 15 min at 277 K and resuspended in binding buffer (20 m*M* Tris–HCl pH 8.0, 300 m*M* NaCl) containing 0.1% Triton X-100 and 10 m*M* β-mercaptoethanol. The cells were sonicated on ice, the lysate was collected by centrifugation at 18 000*g* for 40 min at 277 K and the pellet was discarded. The supernatant was loaded onto a gravity-flow column (Bio-Rad, USA) packed with 3 ml Glutathione Sepharose 4B resin (GE Healthcare) and the resin was extensively washed with binding buffer. Proteins were eluted from the resin with elution buffer (20 m*M* Tris–HCl pH 8.0, 300 m*M* NaCl, 10 m*M* reduced glutathione). The fusion protein was cleaved overnight with TEV protease at 293 K and then concentrated to 3 ml using a 5 kDa cutoff membrane (Amicon Ultra-15 filter, Millipore, USA). Size-exclusion chromatography was performed using HiLoad 16/60 Superdex 200 (GE Healthcare) pre-equilibrated with wash buffer (20 m*M* Tris–HCl pH 8.0, 50 m*M* NaCl, 1 m*M* DTT, 10% glycerol). The purified protein was concentrated to 10 mg ml^{-1} using a 5 kDa cutoff membrane (Amicon Ultra-15 filter, Millipore, USA).

2.2. Crystallization and X-ray data collection

Initial conditions for crystallization were screened at 293 K by the hanging-drop vapour-diffusion technique using a PEG screening kit from our laboratory which was designed for the crystallization of protein–protein complexes. Protein solution (1 µl) was mixed with reservoir solution (1 µl) and equilibrated against 400 µl reservoir solution. Data sets were collected using a Rayonix MX-225HE CCD detector supported by NSRRC on the BL44XU beamline at SPring-8 (Harima, Japan). The diffraction data were indexed, integrated, scaled and merged using *HKL*-2000 (Otwinowski & Minor, 1997).

3. Results and discussion

The human MST2 SARAH domain was overproduced and purified to homogeneity (approximately 95% purity) using Glutathione Sepharose 4B and Superdex 200 columns. The protein was concentrated to 10 mg ml^{-1} for crystallization trials. Crystals were obtained using many different initial conditions. Crystallization conditions were optimized by changing the concentrations of various salts at 293 K. Crystals diffracting to 2.7 Å resolution were obtained using a reservoir solution consisting of 20%(*m*/*v*) PEG 3350, 1 *M* urea and 0.1 *M* Tris–HCl pH 7.4. The crystals belonged to space group *P*2, with unit-cell parameters a = 62.0, b = 119.2, c = 62.0 Å, α = 90.0, β = 90.5, γ = 90.0°. Assuming the presence of eight molecules as dimers in the asymmetric unit, the Matthews coefficient (V_M) and solvent content were calculated as 2.5 Å^3 Da^{-1} and 50.8%, respectively (Matthews, 1968). Another crystal form was obtained from a solution consisting of 10%(*m*/*v*) PEG 3350, 0.1 *M* ammonium phosphate and 0.1 *M* Tris–HCl pH 7.4 (Fig. 1). The crystals diffracted to 3.0 Å resolution and belonged to space group $P6_122$, with unit-cell parameters a = 54.5, b = 54.5, c = 303.1 Å (Fig. 2). Assuming the presence of two molecules as a dimer in the asymmetric unit, the V_M value was 2.84 Å^3 Da^{-1}

Table 1
Summary of data-collection statistics.

Values in parentheses are for the highest resolution shell.

Temperature (K)	90	90
Oscillation range (°)	1	1
Space group	*P*2	$P6_122$
Unit-cell parameters (Å, °)	a = 62.0, b = 119.2, c = 62.0, α = 90.0, β = 90.5, γ = 90.0	a = 54.5, b = 54.5, c = 303.1
Resolution range (Å)	2.7	3.0
Unique reflections	92874	187965
Multiplicity	3.7	2.1
Completeness (%)	99.8	98.9
R_{merge}† (%)	0.057	0.053
Mean $I/\sigma(I)$	10.4	11.7

† $R_{merge} = \sum_{hkl}\sum_i |I_i(hkl) - \langle I(hkl)\rangle| / \sum_{hkl}\sum_i I_i(hkl)$, where $I_i(hkl)$ is the observed intensity and $\langle I(hkl)\rangle$ is the mean intensity of the reflection.

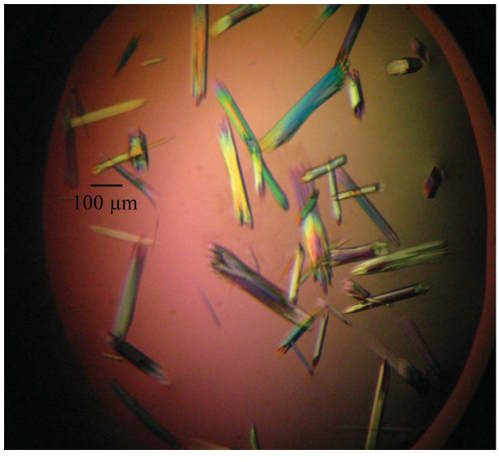

Figure 1
MST2 SARAH domain crystals ($P6_122$ form) grew to maximum dimensions after 3 d.

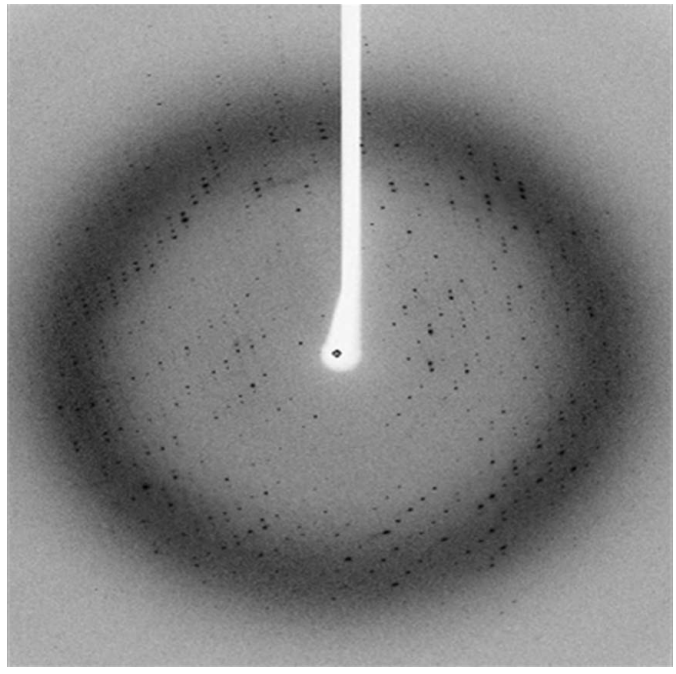

Figure 2
Single-shot image of the diffraction pattern of an MST2 SARAH domain crystal. The best crystal was obtained using 10%(*m*/*v*) PEG 3350, 0.1 *M* ammonium phosphate, 0.1 *M* Tris–HCl pH 7.4 and was flash-cooled in reservoir solution containing 20% PEG 400 as a cryoprotectant.

with a solvent content of 56.7%. The crystallographic parameters and diffraction data statistics are summarized in Table 1. Molecular replacement was attempted with *PHENIX* (Afonine *et al.*, 2005) using the NMR structure of the MST1 SARAH domain as a search model (PDB entry 2jo8; Hwang *et al.*, 2007). Unfortunately, no solution could be found.

The solution structure of the MST1 SARAH domain was reported to be a homodimer (Hwang *et al.*, 2007). Based on our size-exclusion chromatography results, the molecular mass of the purified MST2 SARAH domain was estimated to be 23 kDa, which corresponds to a tetramer (data not shown). Therefore, we wondered whether a tetrameric form of the protein could be observed in the X-ray structure. Hence, determination of the crystal structure of the MST2 SARAH domain could provide further information about the mechanism underlying heterotropic interactions in the Hippo pathway facilitated by SARAH domains. We have prepared selenomethionine-labelled crystals in order to solve the phase problem using anomalous dispersion techniques.

This research was supported by a National Research Foundation of Korea (NRF) grant (2011-0017405) funded by the Korean Government (MEST), the Basic Science Research Program (2010-0003522) through the National Research Foundation of Korea (NRF) and the Korea Healthcare Technology R&D Project (A092006).

References

Afonine, P. V., Grosse-Kunstleve, R. W. & Adams, P. D. (2005). *Acta Cryst.* D**61**, 850–855.
Bao, Y., Hata, Y., Ikeda, M. & Withanage, K. (2011). *J. Biochem.* **149**, 361–379.
Callus, B. A., Verhagen, A. M. & Vaux, D. L. (2006). *FEBS J.* **273**, 4264–4276.
Chan, E. H., Nousiainen, M., Chalamalasetty, R. B., Schäfer, A., Nigg, E. A. & Silljé, H. H. (2005). *Oncogene*, **24**, 2076–2086.
Creasy, C. L., Ambrose, D. M. & Chernoff, J. (1996). *J. Biol. Chem.* **271**, 21049–21053.
Creasy, C. L. & Chernoff, J. (1995). *Gene*, **167**, 303–306.
Graves, J. D., Gotoh, Y., Draves, K. E., Ambrose, D., Han, D. K., Wright, M., Chernoff, J., Clark, E. A. & Krebs, E. G. (1998). *EMBO J.* **17**, 2224–2234.
Hwang, E., Ryu, K.-S., Pääkkönen, K., Güntert, P., Cheong, H.-K., Lim, D.-S., Lee, J.-O., Jeon, Y. H. & Cheong, C. (2007). *Proc. Natl Acad. Sci. USA*, **104**, 9236–9241.
Lee, J.-H., Kim, T.-S., Yang, T.-H., Koo, B.-K., Oh, S.-P., Lee, K.-P., Oh, H.-J., Lee, S.-H., Kong, Y.-Y., Kim, J.-M. & Lim, D.-S. (2008). *EMBO J.* **27**, 1231–1242.
Matthews, B. W. (1968). *J. Mol. Biol.* **33**, 491–497.
Otwinowski, Z. & Minor, W. (1997). *Methods Enzymol.* **276**, 307–326.
Scheel, H. & Hofmann, K. (2003). *Curr. Biol.* **13**, R899–R900.
Wu, S., Huang, J., Dong, J. & Pan, D. (2003). *Cell*, **114**, 445–456.
Zhao, B. *et al.* (2007). *Genes Dev.* **21**, 2747–2761.